# Exchange Splitting of Epitaxial fcc Fe/Cu(100) versus bcc Fe/Ag(100)

F. J. Himpsel

*IBM Research Division, Thomas J. Watson Research Center, P.O. Box 218, Yorktown Heights, New York 10598*

The magnetic exchange splitting of epitaxial Fe films is determined using inverse photoemission. fcc Fe grown on Cu(100) is found in two phases, one obtained by deposition at 300 K with a splitting of 1.2 eV, and the second with a splitting of 0.9 eV obtained after annealing above 450 K. bcc Fe on Ag(100) exhibits a splitting of 1.8 eV, similar to that of bulk Fe. The magnetic splitting of the $3d$ states is shown to be correlated linearly with the local magnetic moment, with a slope of 1 eV/$\mu_B$. This relation holds not only for ferromagnets, but also for antiferromagnets, spin glasses, and the free atoms.

The magnetism of thin films has been an exciting and controversial area. Magnetic properties of a few atomic layers turn out to be very sensitive to strain, interaction with the substrate, and temperature [1-4]. Therefore, one hopes it might be possible to tailor the magnetic behavior of atomic layer films and superlattices in the future, when their growth can be brought under complete control. While magnetism has been the central focus of previous work, the underlying electronic band structure remains somewhat of a gray area. The single most important band property related to magnetism is the magnetic exchange splitting of the states near the Fermi level, i.e., the $3d$ states in our case. There have been searches for the exchange splitting in Ni [5], Co [6], and Fe [2,4,7] films with mixed results. In particular, the existence of a splitting of the Fe $3d$ states for the interesting fcc phase of Fe on Cu(100) has been controversial [2], despite the fact that Fe has a bulk exchange splitting larger than Co and Ni. One of the experimental problems in determining the $3d$ splitting is the overlap between different $d$ bands, which makes it difficult to separate majority and minority components of the same band. In the classical $3d$ ferromagnets, one has more $d$ bands occupied than unoccupied. Thus the problem can be alleviated by probing unoccupied bands with inverse photoemission, instead of occupied bands with photoemission. This has been demonstrated [8] for bulk Fe(100). The work reported here shows that the exchange splitting can be resolved for thin Fe films and that it depends on the structure. Not only do fcc films exhibit a splitting different from bcc films, they also undergo an irreversible phase transition into a second fcc phase upon annealing. These phases tie in well with magnetic phases observed previously [1,2].

The magnetic thin-film systems chosen here, i.e., fcc Fe/Cu(100) and bcc Fe/Ag(100), stand out as some of the best-characterized [1-4] examples. They have a certain tutorial value, since the band structure of Fe can be studied in the bcc and fcc phases. Only very few such examples have been studied. The bcc Fe(100) surface is lattice matched within 1% of the fcc Ag(100) surface since the cubic lattice constant of Ag (4.08 Å) is about a factor of $\sqrt{2}$ times that of Fe (2.86 Å). The extra face-centered atom on the Ag(100) surface makes up for the factor of 2 larger surface unit cell. The fcc phase of Fe in the ferromagnetic state has its energy minimum at a lattice constant close to that of fcc Cu (3.61 Å), according to first-principles calculations [9]. Relative to the bcc phase the atomic volume is expanded. In general, one would expect an increase of the magnetic moment when diluting the Fe atoms, since one has a large moment of $4\mu_B$ in the atomic limit, due to Hund's rule. Calculations [9], however, produce a low-spin phase ($\approx 1\mu_B$) in addition to the expected high-spin phase ($\approx 2.5\mu_B$), while bcc Fe has a moment in between ($2.2\mu_B$). A further complication arises from the paramagnetic and antiferromagnetic phases of fcc Fe, which have a smaller calculated equilibrium volume, even less than bcc Fe. At the lattice spacing of Cu(100) these phases are still quite competitive with the ferromagnetic phase. Indeed, the variety of seemingly conflicting magnetic data on this system can be reconciled by assuming a metastable ferromagnetic phase for low-temperature deposition, which converts into an antiferromagnetic phase upon annealing to about 450 K, with a possible ferromagnetic surface layer. The phase diagram becomes even richer for films thinner than three layers, with the Curie temperature and spin orientation depending on the film thickness. Here, we will concentrate on the simpler, bulklike properties of films more than three layers thick.

The exchange splitting is resolved in Fig. 1 for bcc Fe grown epitaxially on Ag(100) at room temperature [deposition rate 8 Å/min at a pressure in the $10^{-10}$-Torr range; thickness 15 Å, i.e., ten bcc Fe(100) layers]. It is similar to that of bulk Fe(100). The epitaxial film does not order as well as the bulk, which is reflected in the weakness of the image surface state and the lower intensity of the majority $d$ band at the Fermi level. The same phenomena are observed for a Fe film grown homoepitaxially on Fe(100) at room temperature (not shown). In both cases, the LEED pattern exhibits large oscillations of the spot width with energy, indicating many small terraces. While the homoepitaxially grown Fe film can be annealed to give a bulklike spectrum, the Fe film on Ag(100) is affected by Ag segregation before it can order properly.
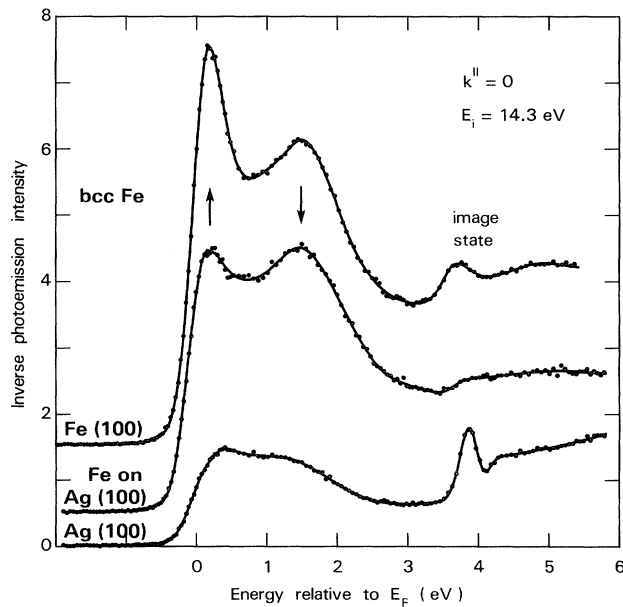
FIG. 1. Inverse photoemission spectrum for ten layers of bcc Fe grown epitaxially on Ag(100), showing the magnetic exchange splitting of the uppermost $3d$ band (see arrows). It is similar to that of bulk bcc Fe.
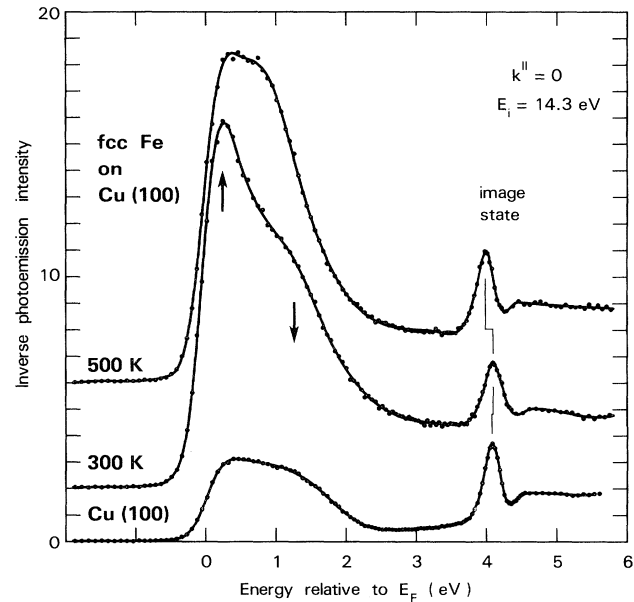


FIG. 2. Inverse photoemission spectra for eight layers of fcc Fe grown epitaxially on Cu(100). The magnetic exchange splitting (see arrows) is smaller than that of bcc Fe, and collapses further after a second, stable phase is reached by annealing to 500 K. The experimental conditions are identical to those for bcc Fe in Fig. 1 [thickness 15 Å, electrons incident normal to the (100) face at an energy of 14.3 eV].

Inverse photoemission spectra for fcc Fe grown epitaxially on Cu(100) are shown in Fig. 2 (thickness again 15 Å, corresponding to eight fcc Fe layers at the Cu lattice constant). The growth morphology is better than on Ag(100), as indicated by the intense and sharp image state. It becomes as sharp as that of the Cu(100) substrate after annealing to 500 K. The LEED pattern shows a 1×1 structure with weak, intensity-modulated streaks along the [10] and [01] directions, consistent with previously reported 5×1 reconstructions. For fcc Fe on Cu(100) one can clearly distinguish two phases. A metastable phase obtained at room-temperature deposition converts irreversibly to a second phase at about 400 K. The latter is stable beyond 500 K, where Cu diffuses out and covers the Fe film. The work function of the metastable room-temperature phase is 0.13 eV higher than that of the annealed phase and 0.02 eV higher than that of Cu(100) (∼4.6 eV). This can be inferred from the shift of the image state (Fig. 2), which is tied to the vacuum level. The most striking feature of the annealed phase is a collapse of the exchange splitting (see arrows for the majority and minority spin $3d$ bands in Fig. 2). This could be due to the onset of antiferromagnetic ordering, coupled with a lower local moment. These characteristics are observed for the whole thickness range from one to eight fcc Fe(100) layers studied here.

The exchange splittings in Figs. 1 and 2 can be quantified by fitting with two Lorentzians of equal area, cut off by the Fermi function, and convoluted with the known resolution function of the inverse photoemission system (0.26 eV FWHM at low energies). Another way is to divide out the Fermi cutoff and look for minima in the second derivative. The resulting splittings for fcc Fe/Cu(100) are $1.2 \pm 0.1$ eV at 300 K and $0.9 \pm 0.05$ eV after annealing to 500 K (and cooling back to 300 K for taking the data). For bcc Fe/Ag(100) and for bulk Fe(100) the two peaks are 1.6 eV apart. However, the majority state lies below the Fermi level, as indicated by its small area. At lower electron energies the two states move up and the areas become equal, giving the true magnetic splitting of 1.8 eV (not shown, compare Ref. [8] for bulk Fe). This truncation problem does not arise for fcc Fe/Cu(100), where the splitting is independent of the electron energy.

The observed splittings correspond to well-defined bands at particular points in momentum space. These can be inferred from the band topology that is well known from bulk band calculations [8–13]. For bcc Fe/Ag(100) and Fe(100) one samples the $H'_{25}$ critical point (see Santoni and Himpsel, Ref. [8]). For fcc Fe/Cu(100) there is only one dipole-allowed $d$ band above the Fermi level at normal incidence, i.e., the section of the $\Delta_5$ band in the outer half of the Brillouin zone (for details see Ref. [10]).

To put the results for thin Fe films into perspective it is useful to compare them with the splittings and magnetic moments of the bulk $3d$ ferromagnets Fe, Co, and Ni (Fig. 3 and Refs. [8,11]). It turns out that there is a
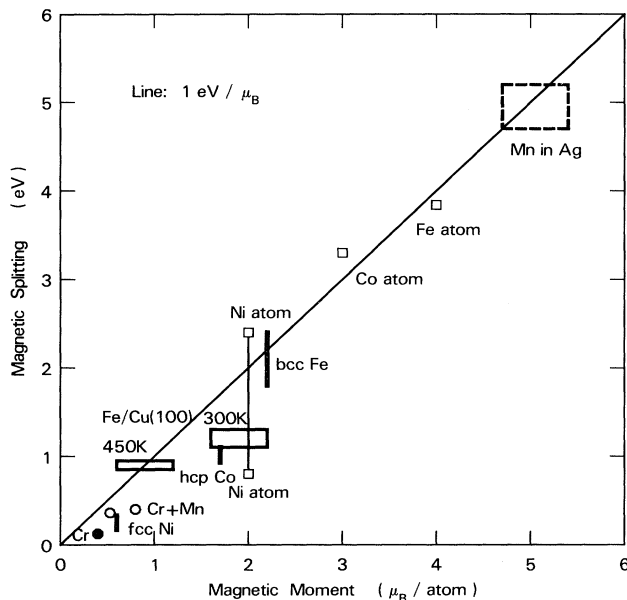
FIG. 3. Correlation between the magnetic exchange splitting of the $3d$ states and the local magnetic moment. The two quantities are roughly proportional with a slope of $1$ eV/$\mu_B$. The data for ferromagnetic Fe, Co, and Ni are from Refs. [8,11], for antiferromagnetic Cr from Ref. [16], for the spin glass Mn in Ag from Ref. [17], and for the free atoms from Ref. [18]. The results of this work on fcc Fe/Cu(100) fit into the picture when combined with the data of Ref. [14] on the magnetic moment.

correlation between the splitting and the magnetic moment, with roughly 1-eV splitting per Bohr magneton $\mu_B$ for large moments and somewhat less for small moments. The data for fcc Fe/Cu(100) fit into this picture when using a previous measurement [14] of the moment. In this work a moment of $1.9\mu_B$/atom is found for three layers of Fe deposited at 125 K, which collapses to $0.9\mu_B$/atom when growing at elevated temperature (350 K). One should keep in mind, though, that the detailed growth conditions are different in the two experiments. It is surprising that this simple proportionality of 1 eV/$\mu_B$ between exchange splitting and moment can be extended beyond the realm of ferromagnets. As Fig. 3 shows, it appears to be valid for antiferromagnets [15,16] (such as Cr and Mn-doped Cr), spin glasses [17] (such as Mn in Ag), and even for the free atoms [18]. Long-range, ferromagnetic ordering seems to be irrelevant for the exchange splitting. Only the local magnetization at a given atomic site counts. This type of measurement is still possible in magnetically disordered systems and could be useful to estimate the local magnetic moment from the exchange splitting [19]. Such a situation might occur for monolayers of magnetic materials [20].

A relation between the exchange splitting and the moment is expected in the context of itinerant ferromagnets [12]. The ratio of the exchange splitting at the Fermi level to the moment is known as the Stoner parameter

[see Eq. (2.14) in Ref. [12]]. It is essential in determining the magnetic properties, such as Curie temperature, magnetization, and susceptibility, at least in a simple Stoner model. Independent of that model one finds that more sophisticated local-density calculations [12,13] give a ratio of splitting to moment in the range of 0.9 and 1.0 eV/$\mu_B$ for ferromagnetic $3d$ metals, nearly independent of the material and close to the average slope of 1 eV/$\mu_B$ found experimentally [21]. The more general, empirical correlation in Fig. 3 poses an interesting challenge to first-principles theory, i.e., to understand its origin and to point out the limitations for determining local moments from the splitting.

[1] For recent structural and magnetic work on Fe/Cu(100), see M. Onellion, M. A. Thompson, J. L. Erskine, C. B. Duke, and A. Paton, Surf. Sci. **179**, 219 (1987); S. A. Chambers, T. J. Wagener, and J. H. Weaver, Phys. Rev. B **36**, 8992 (1987); W. Daum, C. Stuhlmann, and H. Ibach, Phys. Rev. Lett. **60**, 2741 (1988); C. Liu, E. R. Moog, and S. D. Bader, Phys. Rev. Lett. **60**, 2422 (1988); W. A. A. Macedo and W. Keune, Phys. Rev. Lett. **61**, 475 (1988); S. H. Lu, J. Quinn, D. Tian, F. Jona, and P. M. Marcus, Surf. Sci. **209**, 364 (1989); D. P. Pappas, K.-P. Kämper, and H. Hopster, Phys. Rev. Lett. **64**, 3179 (1990); H. Glatzel, Th. Fauster, B. M. U. Scherzer, and V. Dose (to be published).

[2] For results on the magnetic splitting of Fe/Cu(100), see A. A. Hezaveh, G. Jennings, D. Pescia, R. F. Willis, K. Prince, M. Surman, and A. Bradshaw, Solid State Commun. **57**, 329 (1986); M. F. Onellion, C. L. Fu, M. A. Thompson, J. L. Erskine, and A. J. Freeman, Phys. Rev. B **33**, 7322 (1986); H. I. Starnberg, M. T. Johnson, D. Pescia, and H. P. Hughes, Surf. Sci. **178**, 336 (1986); P. A. Montano, G. W. Fernando, B. R. Cooper, E. R. Moog, H. M. Naik, S. D. Bader, Y. C. Lee, Y. N. Carici, H. Min, and J. Marcano, Phys. Rev. Lett. **59**, 1041 (1987); C. Carbone, G. S. Sohal, E. Kisker, and E. F. Wassermann, J. Appl. Phys. **63**, 3499 (1988); J. G. Tobin, M. K. Wagner, X.-Q. Guo, and S. Y. Tong (to be published); D. P. Pappas, K.-P. Kämper, B. P. Miller, H. Hopster, D. E. Fowler, C. R. Brundle, A. C. Luntz, and Z.-X. Shen, Phys. Rev. Lett. **66**, 504 (1991).

[3] For recent structural and magnetic work on Fe/Ag(100), see B. Heinrich, K. B. Urquhart, A. S. Arrott, J. F. Cochran, K. Myrtle, and S. T. Purcell, Phys. Rev. Lett. **59**, 1756 (1987); M. Stampanoni, A. Vaterlaus, M. Aeschlimann, and F. Meier, Phys. Rev. Lett. **59**, 2483 (1987); H. Li, Y. S. Li, J. Quinn, D. Tian, J. Sokolov, F. Jona, and P. M. Marcus, Phys. Rev. B **42**, 9195 (1990).

[4] For results on the magnetic splitting of Fe/Ag(100), see B. T. Jonker, K.-H. Walker, E. Kisker, G. A. Prinz, and C. Carbone, Phys. Rev. Lett. **57**, 142 (1986).

[5] M. A. Thompson and J. L. Erskine, Phys. Rev. B **31**, 6832 (1985); K.-P. Kämper, W. Schmitt, D. A. Wesner, and G. Güntherodt, Appl. Phys. A **49**, 573 (1989).

[6] R. Miranda, F. Ynduráin, D. Chandesris, J. Lecante, and

Y. Petroff, Surf. Sci. **117**, 319 (1982); Phys. Rev. B **25**, 527 (1982); R. Miranda, D. Chandesris, and J. Lecante, Surf. Sci. **130**, 269 (1983); C. M. Schneider, J. J. de Miguel, P. Bressler, J. Garbe, S. Ferrer, R. Miranda, and J. Kirschner, J. Phys. (Paris) **49**, 1657 (1988).

[7] Qing Cai, G. J. Lapeyre, and R. Avci, J. Appl. Phys. **67**, 4916 (1990); Mater. Res. Soc. Symp. Proc. **151**, 65 (1989); W. Heinen, C. Carbone, T. Kachel, and W. Gudat, J. Electron Spectrosc. **51**, 701 (1990); J. Quinn, Y. S. Li, D. Tian, F. Jona, and P. M. Marcus, Phys. Rev. B **43**, 3959 (1991).

[8] J. Kirschner, M. Glöbl, V. Dose, and H. Scheidt, Phys. Rev. Lett. **53**, 612 (1984); A. Santoni and F. J. Himpsel, Phys. Rev. B **43**, 1305 (1991).

[9] J. Kübler, Phys. Lett. **81A**, 81 (1981); C. S. Wang, B. M. Klein, and H. Krakauer, Phys. Rev. Lett. **54**, 1852 (1985); V. L. Moruzzi, P. M. Marcus, K. Schwarz, and P. Mohn, Phys. Rev. B **34**, 1784 (1986).

[10] A band mapping study for fcc Fe/Cu(100) will be published elsewhere. In Figs. 1 and 2 the initial energy $E_i$ has been chosen high enough to have a large $3d$ cross section, as can be seen from the large intensity of the Fe emission compared to that of the Cu and Ag substrates. Thereby one also avoids the $\Delta_1$ $s,p$ band in fcc Fe(100) and Cu(100). It crosses the Fermi level at $E_i = 10.5$ eV in Cu(100).

[11] F. J. Himpsel, J. A. Knapp, and D. E. Eastman, Phys. Rev. B **19**, 2919 (1979); P. Heimann, F. J. Himpsel, and D. E. Eastman, Solid State Commun. **39**, 219 (1981); F. J. Himpsel and D. E. Eastman, Phys. Rev. B **21**, 3207 (1980); F. J. Himpsel and Th. Fauster, Phys. Rev. B **26**, 2679 (1982).

[12] O. Gunnarsson, J. Phys. F **6**, 587 (1976).

[13] V. L. Moruzzi, J. F. Janak, and A. R. Williams, *Calculated Electronic Properties of Metals* (Pergamon, New York, 1978); D. A. Papaconstantopoulos, *Handbook of the Band Structure of Elemental Solids* (Plenum, New York, 1986).

[14] W. Schwarzacher, W. Allison, R. F. Willis, J. Penfold, R. C. Ward, I. Jacob, and W. F. Egelhoff, Jr., Solid State Commun. **71**, 563 (1989). For films thicker than three layers the average magnetic moment is found to collapse in this neutron work. The magnetic splitting seen with inverse photoemission does not change with thickness, however. This difference could be due to the fact that the exchange splitting measures the local moment, which appears to remain constant while the long-range order is partially lost. Macedo and Keune (Ref. [1]) report a small magnetic moment for annealed films of fcc Fe on Cu(100), which is quoted to be of similar magnitude as that of antiferromagnetic fcc Fe precipitates in bulk Cu ($0.7\mu_B$). This value is consistent with the value of ($0.9$

$\pm 0.45)\mu_B$ found by Bennett, Schwarzacher, and Egelhoff, for annealed films, even after taking a factor of 2 reduction in the error bars into account [see W. R. Bennett, W. Schwarzacher, and W. F. Egelhoff, Jr., Phys. Rev. Lett. **65**, 3169 (1990)].

[15] The antiferromagnetic case requires closer attention, since the splitting is associated with a gap between unpolarized bands. This gap occurs at the extra Brillouin-zone boundary induced by the reciprocal-lattice vector of the antiferromagnetic ordering. However, the wave functions at the zone boundary are localized on one spin subsystem and thus resemble those of the ferromagnetic case; e.g., the wave function for spin-up electrons at the spin-up subsite represents the bottom of the gap, which is analogous to the majority spin state in a ferromagnet. Spin-up electrons at the spin-down subsite represent the top of the gap, which is analogous to the minority spin state.

[16] W. C. Koehler, R. M. Moon, A. L. Trego, and A. R. Mackintosh, Phys. Rev. **151**, 405 (1966); A. S. Barker, Jr., B. I. Halperin, and T. M. Rice, Phys. Rev. Lett. **20**, 384 (1968); L. W. Bos and D. W. Lynch, Phys. Rev. B **2**, 4567 (1970).

[17] D. van der Marel, G. A. Sawatzky, and F. U. Hillebrecht, Phys. Rev. Lett. **53**, 206 (1984); R. G. Jordan, W. Drube, D. Straub, and F. J. Himpsel, Phys. Rev. B **33**, 5280 (1986).

[18] For the free atoms the spin magnetic moment is plotted versus the splitting between the strongest lines in the photoelectron spectra that correspond to the ionization of a minority and a majority spin $3d$ electron, respectively. These are $Fe^+ 3d^5 4s^2$: $^6S, ^4G$; $Co^+ 3d^6 4s^2$: $^5D, ^3H$; $Ni^+ 3d^7 4s^2$: $^4F, ^2G$ and $^4P, ^2P,H,D$. The values in Fig. 3 are from M. Meyer, Th. Prescher, E. von Raven, M. Richter, E. Schmidt, B. Sonntag, and H.-E. Wetzel, Z. Phys. D **2**, 347 (1986); E. Schmidt, H. Schröder, B. Sonntag, H. Voss, and H. E. Wetzel, J. Phys. B **16**, 2961 (1983); E. Schmidt, thesis, Hamburg, 1985 (unpublished); see also C. Corliss and J. Sugar, J. Phys. Chem. Ref. Data **10**, 197 (1981); **11**, 135 (1982).

[19] The $3s$ core level can be used in a similar fashion, due to the interaction of the $3s$ hole with the $3d$ states. See D. A. Shirley, in *Photoemission in Solids I*, edited by M. Cardona and L. Ley, Springer Topics in Applied Physics Vol. 26 (Springer, Berlin, 1978), p. 165.

[20] M. T. Kief, G. Mankey, and R. F. Willis (to be published).

[21] A more detailed account of this correlation will be published separately [F. J. Himpsel, J. Magn. Magn. Mater. (to be published)]. The local-density points lie closer to the $1$-eV$/\mu_B$ line than the data in the low-moment region. For the case of Ni the reduced exchange splitting in the data has been understood in terms of many-body effects.